

# Twinning modes in nylon 6.6

D. P. POPE, A. KELLER

*H. H. Wills Physics Laboratory, University of Bristol, Bristol, UK*

The possible twinning modes of nylon 6.6 are predicted on the basis of the crystal structure using Mallard's Law for pseudo-hexagonal lattices. Three conjugate pairs of twin modes are expected. On compression of samples oriented by drawing and strong rolling the main twin mode operative is shown to be  $(1\bar{1}0)$  and evidence is found for at least two other twin modes, probably  $(010)$  and  $(100)$ . These results are used to explain the texture of lightly rolled sheet as a superposition of a twinned component on an untwinned component, and can be further generalized to explain the previously observed texture produced by slight extension of randomly oriented material.

## 1. Introduction

The presence of twinning on extension of unoriented nylon 6.6 was pointed out by Hay and Keller [3] who took it to be  $(110)$  twinning, although this could not be distinguished from other possibilities. The main purpose of this paper is to examine the possible twinning modes using our knowledge of the crystal and molecular structure, and to distinguish between them using oriented samples prepared by drawing and rolling.

The crystal structure of nylon 6.6 has been determined by Bunn and Garner [1] who proposed a triclinic unit cell with hydrogen bonds between molecules in  $(010)$  planes (Fig. 1). This was denoted the  $\alpha$ -structure. A pair of diffraction spots which cannot be indexed on the triclinic unit cell was taken as evidence for a distinct  $\beta$  phase formed by a different method of stacking H-bonded planes, as illustrated in Fig. 2. Bunn and Garner [1] suggest that, in fact, the two forms may be intimately mixed thus explaining the frequently observed layer line streak connecting the  $\alpha$  and  $\beta$  002 reflections. The two sets of spots have also been explained in terms of limited crystal thickness normal to  $(010)$  planes [2], thus obviating the need for two distinct phases.

Recently Chang *et al.* [4] examined the structure of hot-rolled nylon 6.6 using pole figures and found that the chain axes aligned along the roll direction and  $(010)$  planes aligned in the roll plane, giving the texture shown in (Fig. 3a). This implies slip on the H-bonded  $(010)$  planes as would be expected, contrary to

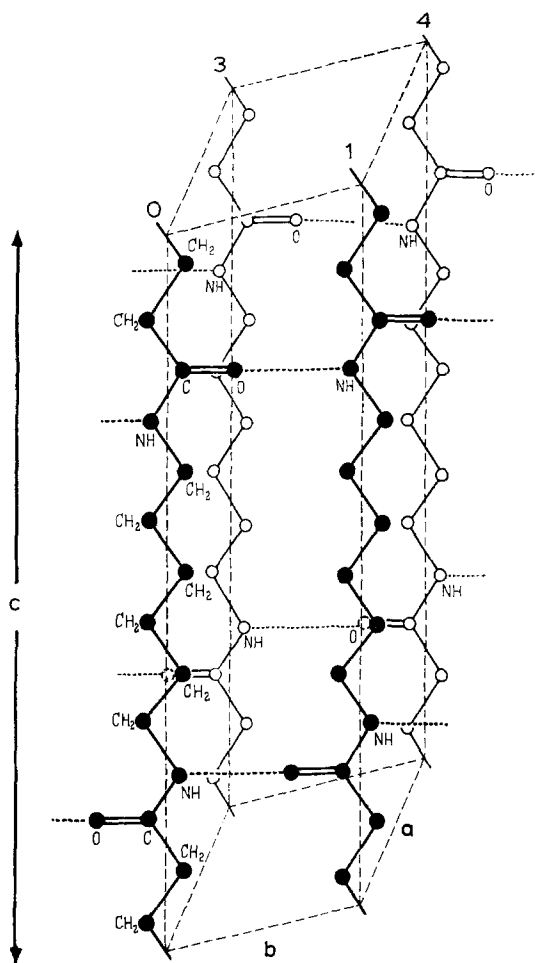
the suggestion of Akahane and Mochizuki [5] that it is the plane of the molecular zigzags which aligns normal to the compression axis. In nylon 6.6 this is the  $(120)$  plane, at  $26^\circ$  to  $(010)$  and its alignment would produce the texture shown in Fig. 3b. During the course of the experiments to be described a texture similar to this was found in some rolled samples, so a further aim of the paper is to explain this texture. As will be shown, it can be interpreted by twinning in the initial stages of rolling, and hence can be explained in crystallographic terms without recourse to molecular considerations.

In addition, the twinned samples revealed that the angle between  $(010)$  and  $(100)$  planes was  $28^\circ$  rather than  $24^\circ$  as predicted by the Bunn and Garner unit cell, and the  $(010)$  spacing was also found to be about 4% larger than predicted. The latter observation was confirmed both in unoriented and in drawn and annealed samples, so it cannot be a consequence of deformation of the unit cell on rolling. As both observations are in agreement with those of Chang *et al.* on hot-rolled samples [4] they appear to be genuine and have been taken into account in predicting orientations in the following sections.

## 2. Derivation of the possible twinning modes

### 2.1. Transverse displacement of the chains

This section follows, with some modifications and additions, the work of Hay [6] who listed the six possible twin modes. For twin planes containing the chain axis, with which we shall be



$$a = 4.9 \text{ \AA}$$

$$b = 5.4 \text{ \AA}$$

$$c = 17.2 \text{ \AA}$$

$$\alpha = 48.5^\circ$$

$$\beta = 77^\circ$$

$$\gamma = 63.5^\circ$$

Figure 1 The unit cell of nylon 6.6, after Bunn and Garner [1].

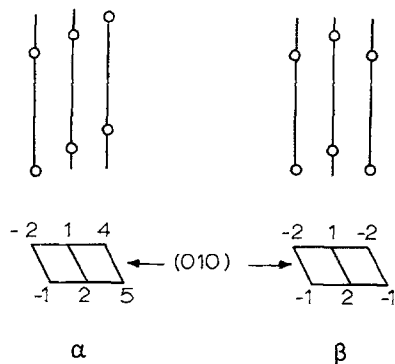


Figure 2 Relation between  $\alpha$  and  $\beta$  forms proposed by Bunn and Garner. The bottom diagrams show projections of the unit cell normal to the  $c$ -axis, the numbers denoting the relative heights of the C-atoms in units of C-C distances along the chain (as in Fig. 1).

solely concerned, these can be deduced by considering the projection of the unit cell on a plane normal to  $c$  and using Mallard's law for pseudo-hexagonal lattices [7]. This states that the twin planes are those planes which would be symmetry planes if the lattice were truly hexagonal. The projection of the nylon 6.6 unit cell on  $[001]$  (Fig. 4) shows that it is pseudo-hexagonal, and that the planes which would be mirror planes in a hexagonal lattice are  $(100)$   $(010)$   $(120)$   $(210)$   $(110)$  and  $(1\bar{1}0)$ . Thus six twin modes can be expected. These form three conjugate pairs and are listed in Table I, together with the plane transformations and the magnitudes of the shears involved, and illustrated in Fig. 5. In this figure, the twin planes are marked by a dashed line and shown oriented at  $45^\circ$ , thus the initial crystal is shown in the optimum orientation for activation of each twin mode by either vertical extension or horizontal compression.

Table II shows the changes in orientation of the  $100$  and  $010$  reflections for optimally oriented crystals for each twin mode. As the experiments to be reported were performed in compression the angles are measured with respect to the compression axis. The calculations were made using the unit cell projection shown

TABLE I The properties of the six possible twin modes are listed. The shear  $\gamma_1$  is the shear on the twin plane normal to the chain axis,  $\gamma_2$  is the shear component parallel to the chain axis, and  $\gamma$  the total shear.

Mode	Major plane transformations	Twin plane	Conjugate plane	Shear $\gamma_1$	Chain rotation	Chain translation in C-C units	Shear $\gamma_2$	Total shear $\gamma$
A } B } C } D } E } F }	(100) ↔ (110)	(010)	(210)	0.30	52°	5	1.7	1.73
		(210)	(010)	0.30	128°	1	0.54	0.62
	(100) ↔ (010)	(1 $\bar{1}$ 0)	(110)	0.21	112°	2	1.1	1.11
		(110)	(1 $\bar{1}$ 0)	0.21	68°	4	1.4	1.41
	(010) ↔ (110)	(100)	(120)	0.06	180°	1	0.29	0.30
		(120)	(100)	0.06	0°	3	1.9	1.9

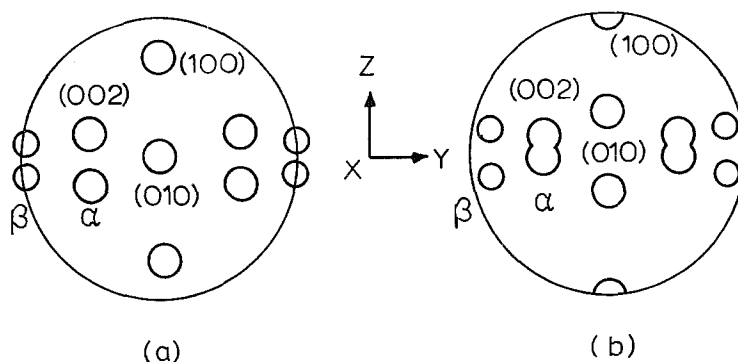


Figure 3 Pole figures of rolled nylon 6.6 expected from (a) (010) slip; (b) alignment of (120) planes. Y is the draw and roll direction and X the sheet normal.

TABLE II Initial and final plane orientations with respect to the compression axis are shown for crystals in the optimum initial orientation for each twin mode. The figures in brackets take into account twin plane rotation due to specimen constraints. (In the case of modes E and F this has a negligible effect.)

Twin mode	Reflection	Initial orientation (°)	Final orientation (°)
A	100	17	73 (81)
	010	45	45 (37)
B	100	10	80 (72)
	010	52	38 (46)
C	100	12	78 (72)
	010	74	16 (10)
D	100	20	70 (76)
	010	82	8 (15)
E	100	45	45
	010	73	17
F	100	46	44
	010	72	18

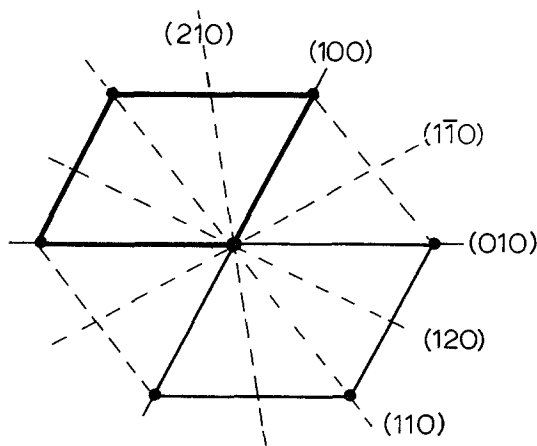


Figure 4 Projection of the unit cell normal to the c-axis to show pseudo-hexagonal symmetry.

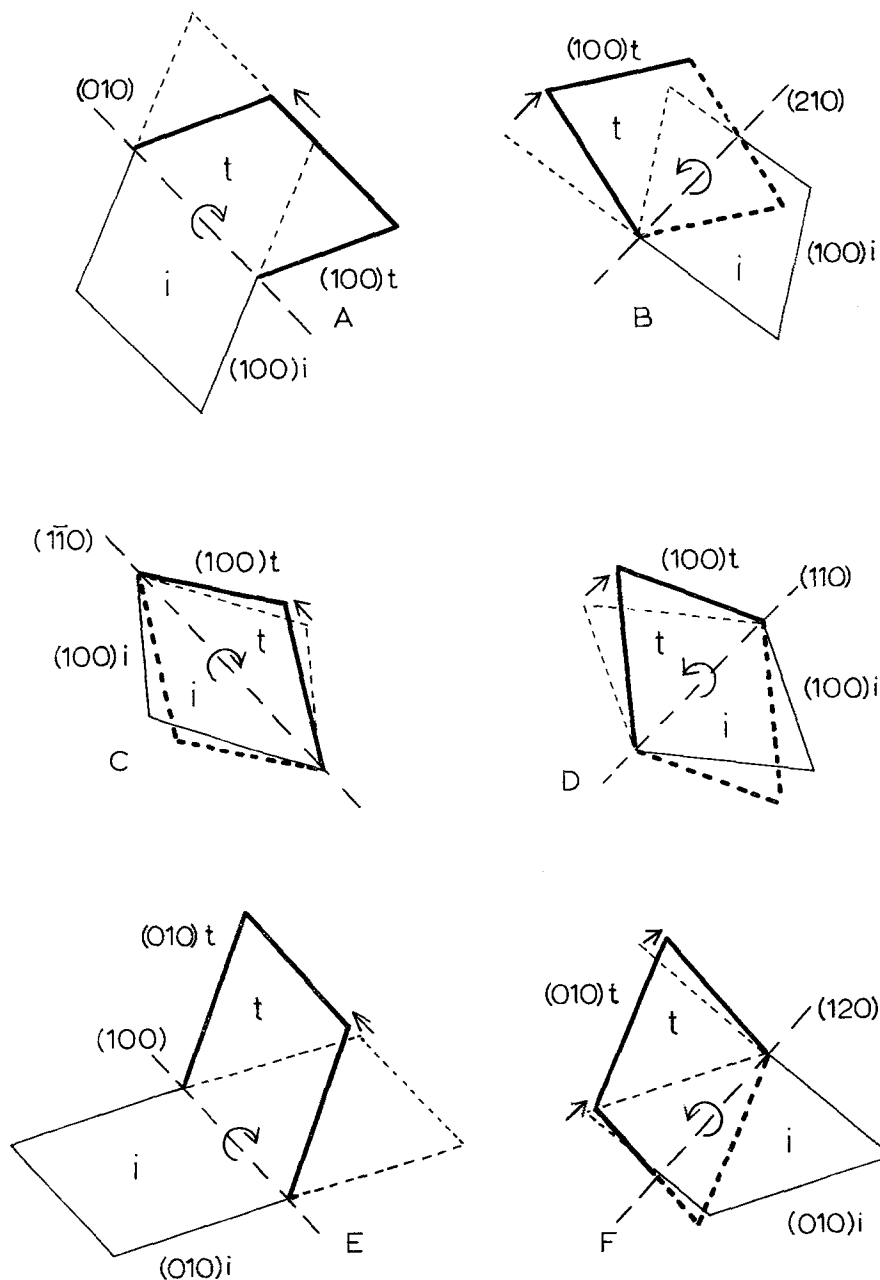


Figure 5 The expected twin modes of nylon 6.6 shown in terms of projections normal to the  $c$ -axis. The initial structures (i) and twinned structures (t) are shown in relation to the twin planes (long dashed lines).

in Fig. 6 which differs slightly from that of Bunn and Garner but fits the observed angle between (010) and (100) planes and the observed (010) spacing, as discussed in the Introduction. These changes in the unit cell parameters make only small differences to the orientation changes on twinning, but alter both the magnitude and the

sense of the shear involved in modes E and F, which if based on the Bunn and Garner cell should be activated by extension rather than compression in the direction concerned.

Allowance should also be made for rotation of the twin plane due to specimen constraints. This rotation is identical in origin to the rotation

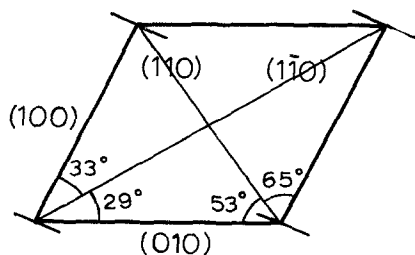


Figure 6 Projection of modified unit cell used to compile Table II. The short lines indicate the molecular planes.

of the slip plane accompanying slip, and its magnitude is given by  $\gamma \sin^2 \alpha$ , where  $\alpha$  is the angle between the twin plane normal and the compression axis and  $\gamma$  the magnitude of the shear. The sense of this rotation is indicated by arrows in Fig. 5 and the (010) and (100) orientations taking it into account are given in brackets in Table II. In practice, the full rotation may not be realized as it will depend on the internal constraints on each crystallite, and some deformation may be accommodated without rotation, especially as in the samples used here two opposing orientations of crystals are always present and there is likely to be a certain amount of disordered material between them.

### 2.2. Longitudinal displacement and rotation of the chains

We have so far been concerned only with the projection of the unit cell on [001], i.e. with transverse rearrangements of the chains. As the unit cell is triclinic, in order to preserve the original structure on twinning, the chains must both rotate and translate along the chain direction. The two twin modes in each conjugate pair have identical effects on the crystal structure, differing only by a rotation. For each conjugate pair the crystal structure can be restored after twinning in two ways, involving complementary rotations and translation on either the twin plane or the conjugate plane. However, for a given mode, translation is more likely to occur on the twin plane as twinning propagates from one twin plane to the next. The necessary rotations and translations are shown in Table I, which also shows the required shear  $\gamma_2$  along the chain direction and the total resultant shear for each twin mode. As an example, the rearrangements involved in modes A and B are shown in Fig. 7.

Each twinning mode, except mode A, involves breaking of the H-bonds. In the case of mode A, these lie in the twin plane, (010), and hence are unaltered by twinning, although they

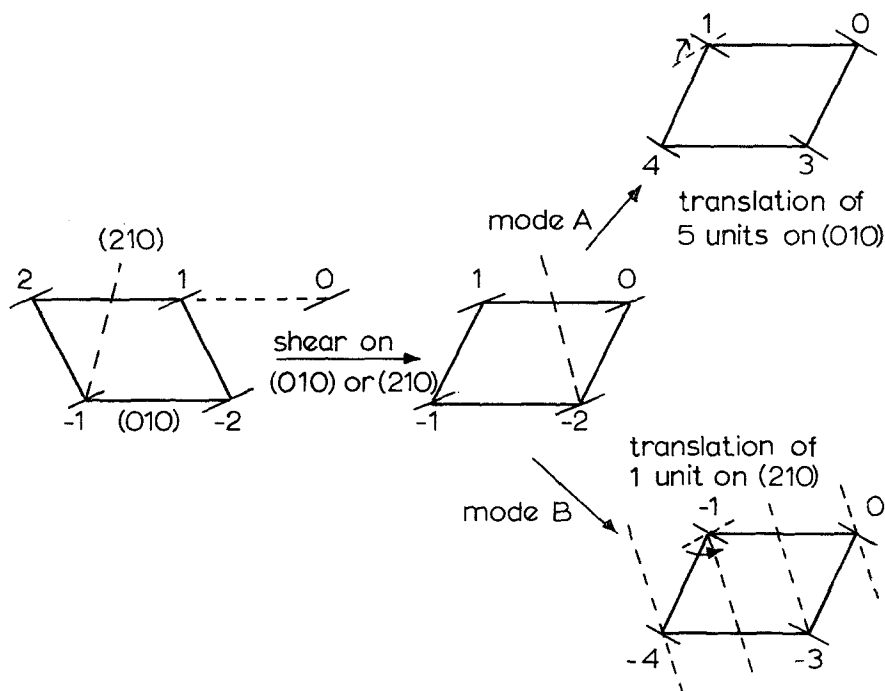


Figure 7 Diagrams to show chain rotations and translations along c-axes required by twinning in modes A and B.

must be disturbed slightly as the chains rotate. In mode B, although the same molecules remain H-bonded, the new H-bonds are formed between different atoms.

Mode A raises the possibility of alternative arrangements of (010) planes, caused by (010) planes translating by less than the five units required to restore the original  $\alpha$  structure. This could lead to an increased proportion of the  $\beta$  phase, or simply a decrease in the regularity of packing of (010) planes which could be interpreted as a decrease in average crystallite thickness.

### 2.3. Factors affecting observed twin modes

The observed twin modes will depend on the relative importance of a number of factors, in particular the amounts of shear and chain rotation involved in each mode and the size of the energy barriers to be overcome in each case. As can be seen from Table I, the modes involving least shear require the larger chain rotations, so it is not a simple matter to make predictions, except that mode A should be preferred as it does not involve rupture of H-bonds.

Another factor which could affect the energetics of twinning is the molecular fold plane, preference being expected for modes in which the twin plane is the fold plane, thus minimizing disturbance of the folds. There is no conclusive evidence regarding the fold plane in nylon 6.6. but from work on single crystals [8] it seems most likely that it should be (010), again favouring mode A.

In a given sample, of course, the twin modes present will depend on the orientations present and their relation to the applied stress direction. In the next section, it will be shown how compression of oriented samples normal to the chain direction enables investigation of all the twin modes discussed above.

## 3. Observation of the twin modes

### 3.1. Experimental and results

Oriented specimens were prepared by drawing at room temperature followed by rolling along the draw direction to  $0.7 \times$  original thickness and annealing at  $200^\circ\text{C}$ . This produces a texture with the chain axis, [001], along the draw direction  $Y$ , and (010) planes lying in the rolling plane  $Y$ - $Z$ . The four unit cell orientations consistent with this texture are shown in Fig. 8. Specimens with this texture were compressed along  $Z$  and

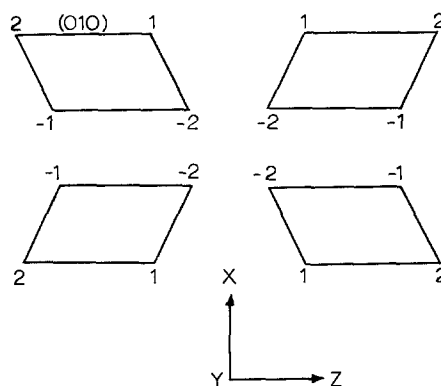


Figure 8 The four unit cell orientations present in drawn and strongly rolled sheet.

X-ray photographs taken with the beam along  $Y$ , thus revealing directly the orientations of the (100) and (010) planes.

The results are shown for various stages of compression in Fig. 9. These X-ray photographs were taken with the sample under stress. Removal of stress caused a certain amount of reversibility, both of specimen dimensions, typically from a strain of 0.30 to 0.25, and of the twinning as revealed by the diffraction patterns. The presence of twinning is clearly indicated by the discontinuous nature of the orientation changes. Comparison of the initial and final textures (Fig. 9a and d) shows that the main twin mode involved must be C or D as the major effect of twinning has been to interchange (010) and (100) planes (see Fig. 5 and Table II). However, the final texture is unexpectedly well defined and a more detailed analysis taking into account the orientation distribution is required.

### 3.2. Analysis of the orientation changes

Fig. 10 shows one of the four texture components (see Fig. 8) subdivided into three different orientation types labelled I, II and III according to the position of their (010) poles in the  $X$ - $Z$  plane. The diagram also indicates, by the appropriate letter, the optimum (010) plane orientation for the activation of each twin mode (see Table II). As the total shear has a component along the chain direction these orientations are not the true optimum positions, which require the stress to be applied at  $45^\circ$  to the resultant shear direction but cannot be realized by the present experimental arrangement.

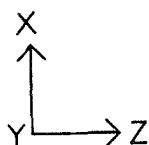
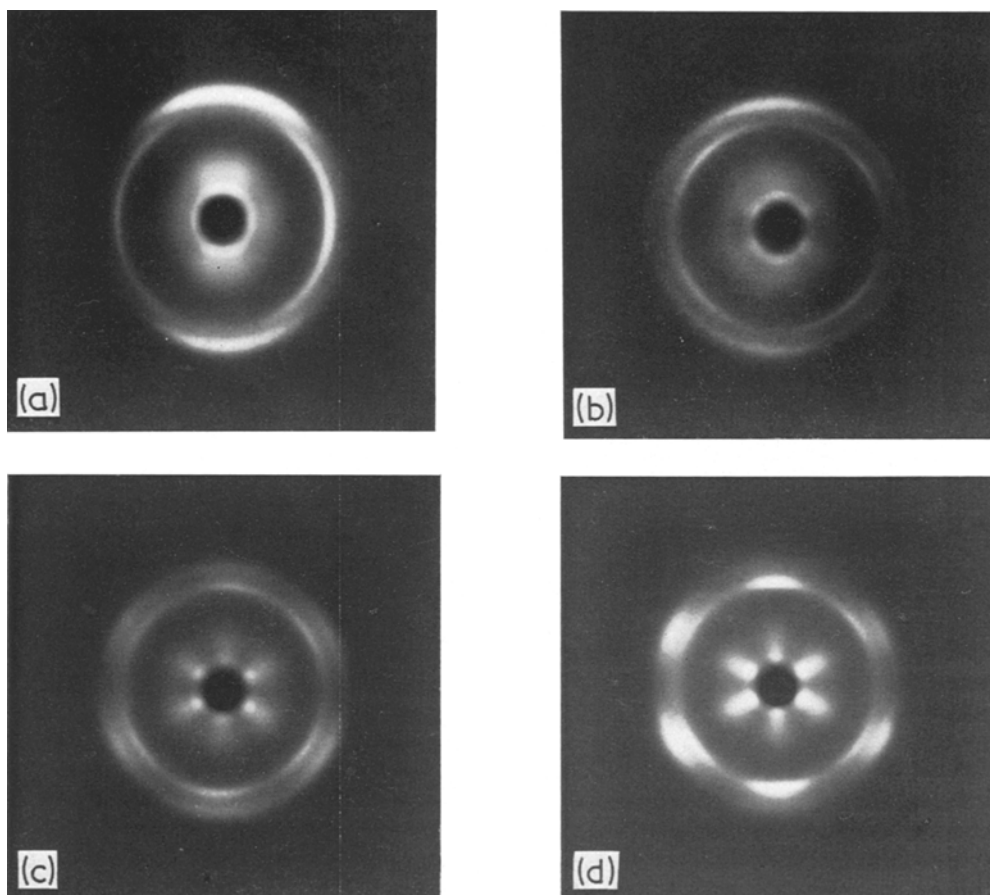


Figure 9 X-ray diffraction patterns of drawn and rolled sheet compressed along Z, beam along Y: (a) zero strain; (b) strain of  $-0.10$ ; (c) strain of  $-0.20$ ; (d) strain of  $-0.30$ . The inner reflection is 100, the outer, 010.

The first sign of twinning, seen in Fig. 9b, is a sharpening of the 010 maximum on X accompanied by the appearance of 010 reflections at about  $50^\circ$  to Z, and removal of (100) poles from Z. This can best be explained by either mode A or mode B acting on crystallites in orientation I. The effects of the two modes are shown in Table IIIa), from which it can be seen that if twin plane rotation is allowed for (figures in brackets), the two modes are indistinguishable. It is not possible from the present evidence to decide which of modes A and B is preferred, especially as the twinned structure is in a position to deform further by (010) slip thus perhaps reducing the observed (010) orientation.

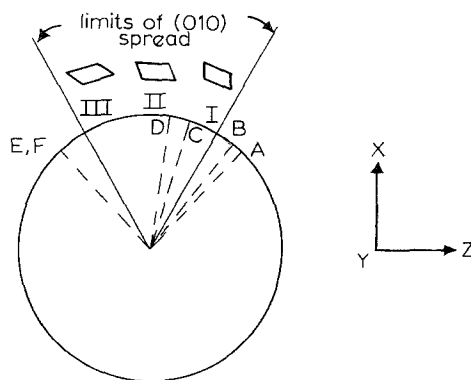


Figure 10 Diagram to show the types of orientation present in drawn and rolled sheet. The letters indicate the optimum (010) orientation for the activation of each twin mode. The diagram shows only one of four mirror-related components (see Fig. 8).

TABLE III The effects of various twinning modes on the orientation of (100) and (010) planes with respect to the compression axis.

Twin mode	Plane	Initial orientation (°)	Final orientation (°)
(a) Effects of modes A and B on crystallites in orientation type I			
A	100	0	56 (68)
	010	62	62 (50)
B	100	0	70 (65)
	010	62	48 (53)
(b) Effects of modes C and D on crystallites in orientation type II			
C	100	28	86 (86)
	010	90	32 (24)
D	100	28	78 (82)
	010	90	17 (21)
(c) Effects of modes E and F on crystallites in orientation type III			
E	100	33	33 (32)
	010	85	29 (30)
F	100	33	31 (33)
	010	85	31 (29)

As deformation proceeds, orientation type II, corresponding to the maximum of the distribution, is affected (Fig. 9c). Table IIIb compares the effects of modes C and D on this orientation. As new (010) poles are observed to form at about 28° to *Z* and new (100) poles at 90°, the best fit is given by mode C, but with less twin plane rotation than expected.

In the final stages of twinning shown in Fig. 9d, the original 010 reflection gradually disappears while the corresponding 100 reflection at about 35° to *Z* remains. This can be explained by mode E or F acting on orientations of type III. The effects of this are shown in Table IIIc for crystallites initially with (010) planes at 5° to the maximum. Again, it is not possible to distinguish between the two modes.

The above conclusions are summarized in Fig. 11, which shows the effects of the various twin modes on one of the four components of the orientation distribution. The presence of at least three twinning modes, each operating on a different part of the orientation range, the maximum of which twins on (1 $\bar{1}$ 0), helps explain why the resulting texture is so well defined as each part of the original texture is twinned to roughly the same final orientation. The definition is probably also improved by (010) slip which will tend

to rotate (010) poles towards *Z* with greatest effect on those oriented at about 45° to *Z*. The crystals resulting from mode A or B twinning of orientation type I are particularly likely to deform by slip.

### 3.3. Discussion

A number of further points should be made, firstly regarding interpretation of the diffraction patterns. As the X-ray beam is directed along *Y* the planes giving rise to the diffraction are those whose normals are tilted out of the *X-Z* plane by the Bragg angle, which is about 10° for (100) and 12° for (010) planes. Thus the beam does not sample the maximum of the distribution. However, photographs taken with the specimen tilted through the Bragg angle yielded nearly identical results as regards the positions of the maxima. In addition, they revealed that the orientation distribution of the twinned crystals is of the form shown in Fig. 12, as would be expected since on compression along *Z* the chains will be constrained to lie in the *X-Y* plane.

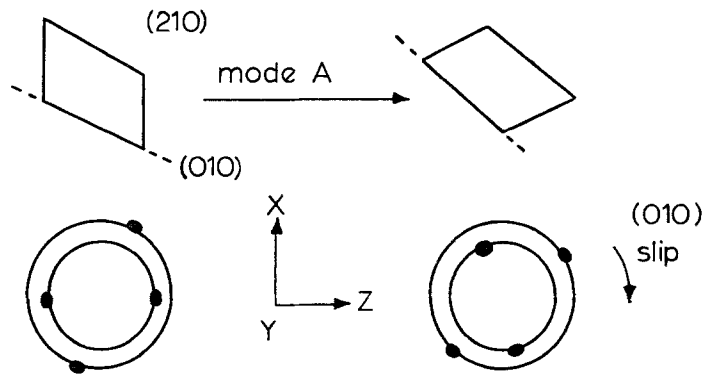
The 002 reflection was observed in both the untwinned and twinned samples and its position was found to have changed as expected. However, in the twinned structure it was less well defined and almost formed a continuous streak with the  $\beta$  reflection. This could well be due to irregular packing of (010) planes, as suggested in Section 2, as a result of mode A twinning.

The strains required to produce the twinned textures shown in Fig. 9c and d are quite large, - 0.2 to - 0.3. If the whole sample were to deform by twinning alone the strain could not exceed - 0.15, therefore other deformation modes must be present, probably crystallographic (010) slip as already mentioned, and deformation of disordered material. Stored energy in the latter could explain the small degree of reversibility observed on removal of pressure. The presence of disordered material could also help explain the reduced amount of twin plane rotation observed at least in the case of mode C (see above), as discussed at the end of Section 2.1.

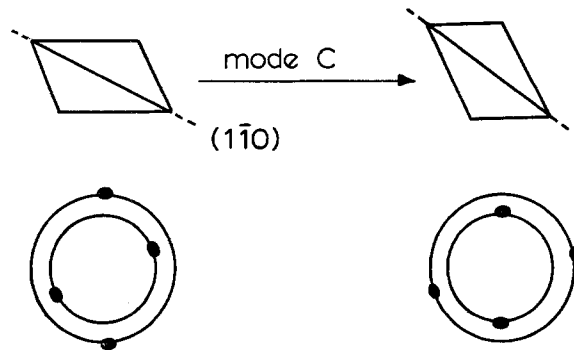
It can be concluded that at least one mode from each conjugate pair of twin modes readily occurs, despite the requirement for breaking of the H-bonds. It is not possible to distinguish between modes A and B or E and F, but mode C occurs in preference to mode D. The fact that crystals most favourably oriented for mode C preferentially twin by mode A or B, shows that



orientation type I



orientation type II



orientation type III

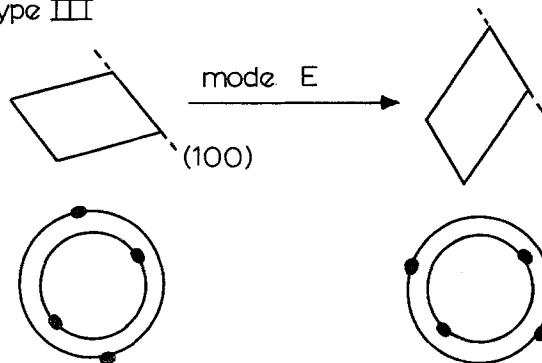


Figure 11 Diagram to show effect of twinning on one component of the original texture and the corresponding X-ray diffraction pattern.

the mode involved, probably mode A, occurs much more readily than C, as expected. Preference between different twin modes, coupled with the orientation factors, results in the three twinning processes occurring in sequence. This

facilitates analysis by allowing the twinning to be separated into three stages involving different components of the orientation distribution, and enabling the conclusions just presented to be reached.

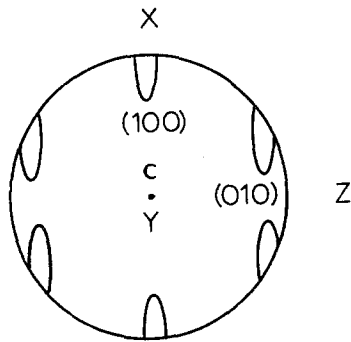


Figure 12 Distribution of (010) and (100) poles in twinned material as deduced from photographs with X-ray beam tilted about Y.

#### 4. Texture of drawn and rolled sheet

Although strong rolling (to about  $0.7 \times$  original thickness or less) produced the texture shown in Fig. 9a, weaker rolling, reducing the thickness to between  $0.9$  and  $0.8 \times$  original thickness, produced the texture shown in Fig. 13\*. As has already been pointed out, this corresponds to alignment of (120) planes, as in Fig. 3b. Such a texture is not expected to result from crystallographic slip as the Burgers vectors for slip on

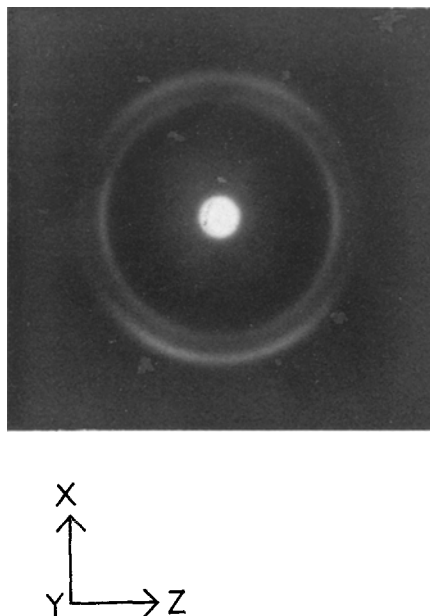


Figure 13 Lightly rolled drawn sheet, showing (010) maxima at  $\sim 28^\circ$  to X.

(120) are large. However, it can be explained in terms of the twinning described in the previous section.

The (010) maxima in Fig. 13 are at about  $28^\circ$  to X, the same angle as made by the (010) poles with the compression direction Z in the twinned oriented material. (On rolling, compression is along X, whereas in the previous section rolled samples were compressed along Z.) Thus the maxima in the rolled sheet could be caused by twinning of crystals with (010) poles originally distributed around Z in the drawn sample. Crystals with (010) poles around X will be unfavourably oriented for any of the twin modes, while those with (010) poles at about  $45^\circ$  to X and Z will twin by modes A or B, which produce only small changes in (010) orientation.

Hence the texture of the rolled sample is essentially a superposition of the texture obtained by uniaxially compressing an oriented sample on a largely unchanged component comprising crystals not suitably oriented for twinning. This is illustrated in Fig. 14. Note that this texture could not be predicted as the result of any one twin mode, but requires the combination deduced in the previous section. This can be verified from Table II – no one twin mode produces a final (010) orientation at  $28^\circ$  to the compression direction. The essential point is that the crystals most favourably oriented for mode C, in fact twin by modes A or B, the (010) maxima being produced by mode C twinning of crystals even less favourably oriented for modes A or B, (cf. Figs. 10 and 11).

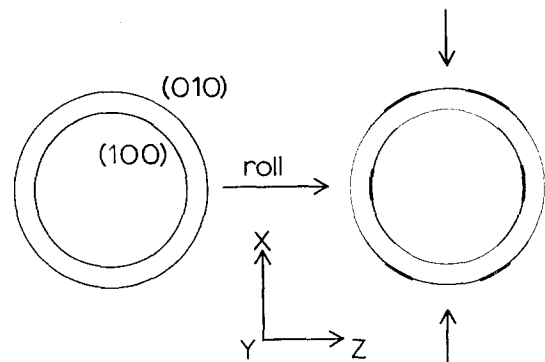


Figure 14 Diagram to show origin of (010) maxima in lightly rolled sheet. The vertical arrows indicate the direction of the compression produced by rolling.

\*The drawn samples showed a certain amount of orientation of (100) and (010) planes around the draw direction owing to the fact that they were in the form of thin strips, in which case grip constraints reproduce the effect of compression normal to the plane of the sheet.

An extension of the above interpretation also explains the texture produced by slight extension of randomly oriented material as reported by Hay and Keller [3]. Those crystals which are suitably oriented twin according to the scheme described in Sections 3 and 4, and the resulting texture is superimposed on the unchanged component of the original textures. This produces a rather marked orientation effect in the  $hk0$  reflections of the diffraction pattern, when viewed normal to the extension axis, similar to that shown in Fig. 13, without, however, affecting the randomness of the  $c$ -axis (chain) orientation.

## 5. Conclusions

Compression of oriented samples of nylon 6.6 produced by drawing and strong rolling has enabled a systematic examination of the twin modes following a preliminary publication on the subject [3]. At least one member of each conjugate pair of twin modes is operative. The main twin mode involved was found to be  $(1\bar{1}0)$ , which operated in preference to  $(110)$ . A distinction between members of the other two conjugate pairs was not possible on experimental grounds, but probably  $(100)$  twinning is preferred to  $(120)$  and  $(010)$  to  $(210)$ . The latter distinction is based on the fact that  $(010)$  twinning is the only mode which does not require breaking of the H-bonds. The observed preference for  $(1\bar{1}0)$  over  $(110)$  remains unaccounted for unless it is due to the influence of the fold plane, in a manner which cannot as yet be specified.

The presence of at least three twin modes,

combined with some  $(010)$  slip, led to a particularly well defined texture, which revealed a discrepancy between the observed angle between  $(010)$  and  $(100)$  planes and that predicted by Bunn and Garner's unit cell. The  $(010)$  spacing was also found to be larger than expected, in agreement with observations of Chang *et al.* [4], so a modified unit cell was used to take account of these observations.

The unusual texture of lightly rolled drawn sheet can be explained by twinning of crystals in one particular orientation range within the transversely isotropic fibre structure, and a similar explanation can account for the initial orientation effects observed on extension of completely isotropic samples [3].

## Acknowledgement

One of us (D.P.P.) is indebted to I.C.I. Ltd for financial support.

## References

1. C. W. BUNN and E. V. GARNER, *Proc. Roy. Soc. A* **189** (1947) 39.
2. A. KELLER and A. MARADUDIN, *J. Phys. Chem. Solids* **2** (1957) 301.
3. I. L. HAY and A. KELLER, *J. Polymer Sci. C* **30** (1970) 289.
4. E. P. CHANG, R. W. GRAY and N. G. MCCRUM, *J. Mater. Sci.* **8** (1973) 397.
5. T. AKAHANE and T. MOCHIZUKI, *J. Polymer Sci. B* **8** (1970) 487.
6. I. L. HAY, Ph.D. Thesis, Bristol University, 1968.
7. F. C. FRANK, *Acta Metallurgica* **1** (1953) 71.
8. P. DREYFUSS and A. KELLER, *J. Macromol. Sci.* **B4** (1970) 811.

Received 15 November and accepted 25 November 1974.